



Universidad  
de Huelva



## Novel results on experimental studies of the $^{46}\text{Mn}$ $\beta^+$ decay channel and its connection to CCSN

D. Godos-Valencia<sup>1,5,\*</sup>, L. Acosta<sup>1,6</sup>, P. Ascher<sup>2</sup>, B. Blank<sup>2</sup>, J. Giovinazzo<sup>2</sup>,  
F. de Oliveira<sup>3</sup>, C. Fougères<sup>4</sup>, A.M. Sánchez-Benítez<sup>5</sup>.

<sup>1</sup>Instituto de Física UNAM, Mexico; <sup>2</sup>LP2i-Bordeaux, France; <sup>3</sup>GANIL, France;

<sup>4</sup>CEA/DAM, France; <sup>5</sup>CEAFMC Universidad de Huelva, Spain,

<sup>6</sup>Instituto de Estructura de la Materia, CSIC, Spain.

(\* dgodosv@gmail.com)



European Nuclear Physics Conference  
September 22, 2025

$^{44}\text{Ti}$  nucleosynthesis

- $^{44}\text{Ti}$  and its eventual decay chain are produced in type II supernovae (CCSN). The photons emitted during the decay chain (67.9, 78.4, 1157 keV) are observed by satellite telescopes for gamma-astronomy (i.e., INTEGRAL), making  $^{44}\text{Ti}$  a good tracer for SN events.
- $^{44}\text{Ti}$  abundance is quite sensitive to the  $^{45}\text{V}(p,\gamma)^{46}\text{Cr}$  reaction rate: the higher the reaction rate [1-3].
- Main objective:** Obtain the energy of new resonant contribution(s) to the  $^{45}\text{V}(p,\gamma)^{46}\text{Cr}$  reaction due to currently unknown excited state(s) of  $^{46}\text{Cr}$ .

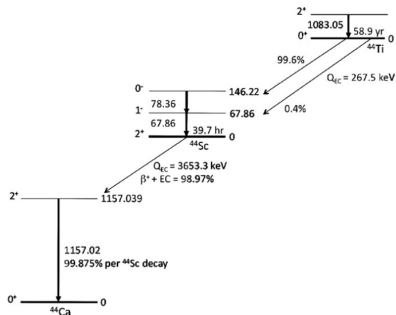


Figura:  $^{44}\text{Ti}$  decay scheme taken from [1].

- [1] L.-S. The, et al., ApJ **504**, 500-515 (1998);
- [2] G. Magkotsios, et al., ApJS **191**, 66-95 (2010);
- [3] K. Hermansen, et al., ApJ **901**, 77:90 (2020)

## $\beta$ -delayed proton emission

$\beta$ -delayed proton emission of <sup>46</sup>Mn allows us to seek excited states of the daughter nucleus <sup>46</sup>Cr and thus, is an indirect method for measuring resonant contributions to the reaction rate of <sup>45</sup>V(p, $\gamma$ )<sup>46</sup>Cr.

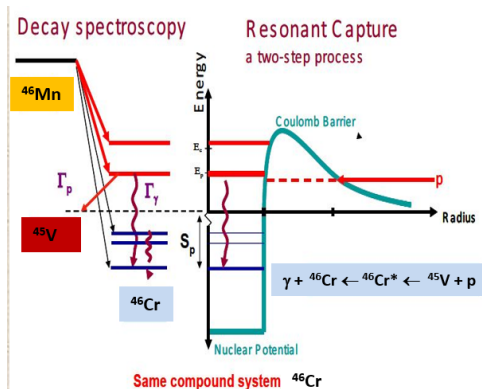
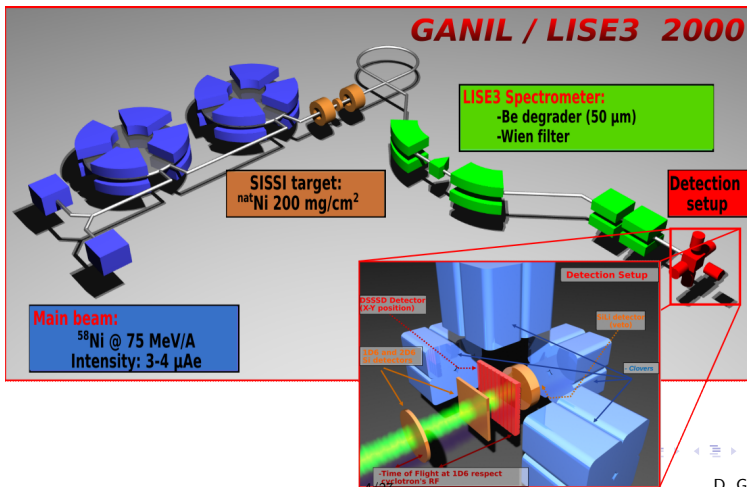


Figura: Adapted from L. Trache, et. al., AIP Conf. Proc 1409-1, 67-70 (2011).

## Beam production at LISE@GANIL for E666 experiment

Data was taken from the experiment “Isospin mixing in pf-shell proton emitters” (Code: E666, Spokesperson: Bertram Blank, from CEN-BG, France) developed using the fragment separator LISE@GANIL (Caen, France).



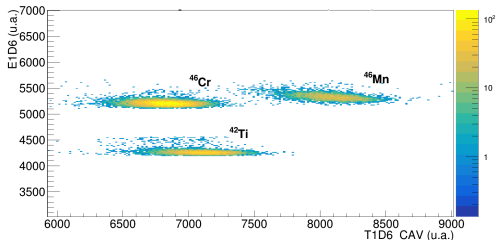
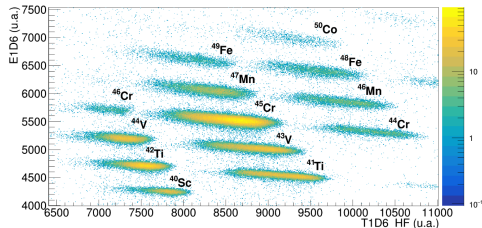
## Experimental analysis

1. As a first step calibrations for the DSSSD X & Y strips, and for the HPGe clover sections were performed.
  - 1.1 For the DSSSD, a triple  $\alpha$ -source ( $^{239}\text{Pm}$ ,  $^{241}\text{Am}$ , and  $^{244}\text{Cm}$ ), and proton emission of well-known nuclei ( $^{49}\text{Fe}$ ,  $^{45}\text{Cr}$ ,  $^{41}\text{Ti}$ , and  $^{50}\text{Co}$ ) were used.
  - 1.2 For the HPGe clovers, we use  $^{56+60}\text{Co}$ ,  $^{207}\text{Bi}$ , and  $^{133}\text{Ba} + ^{137}\text{Cs}$  sources.
2. Later, the ions of interest were selected,  $^{46}\text{Mn}$ , by means of energy loss vs time of flight (ToF) 2D histograms.
3. Finally, decay events corresponding to the  $^{46}\text{Mn}$  were identified using spatial and time correlations between the implantation and the decay signals.



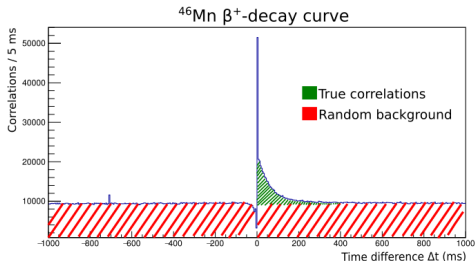
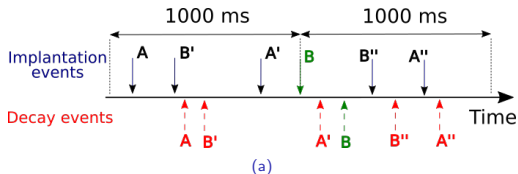
## $^{46}\text{Mn}$ identification

- We use the time of flight (ToF) in the silicon detector to identify the isotope of interest,  $^{46}\text{Mn}$ , among others.
- These events were selected using graphical selection windows.
- More than  $3.15 \times 10^5$  events of  $^{46}\text{Mn}$  were selected during approximately 71.5 hrs of data acquisition.



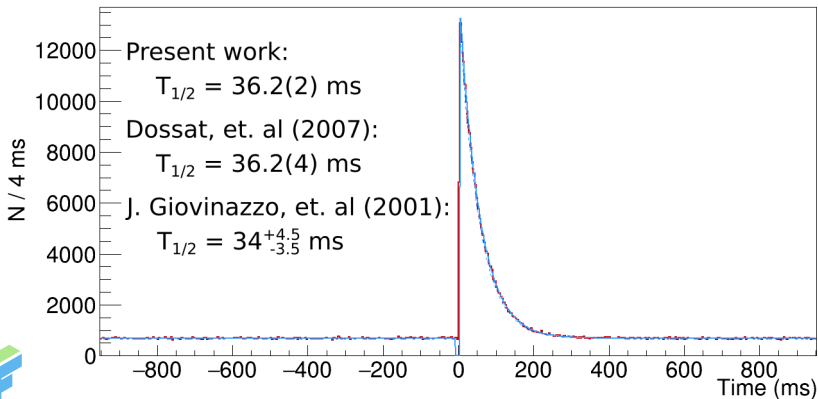
## Time-correlated events

The time correlation between the  $^{46}\text{Mn}$  implantation events and the decay ones were established in the following way:

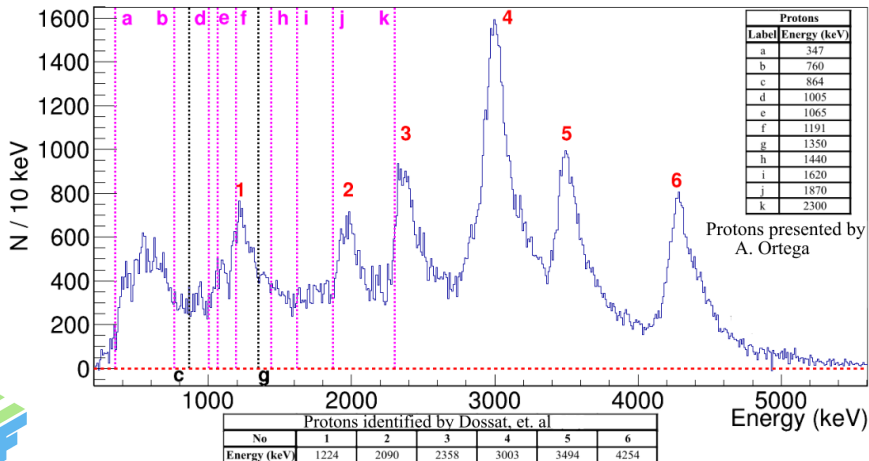


## $^{46}\text{Mn}$ $\beta$ -decay curve

The half-life was obtained using a threshold  $E_{\text{cut}} > 900$  keV, and the systematic error was set with  $E_{\text{cut}} > 1000$  keV.

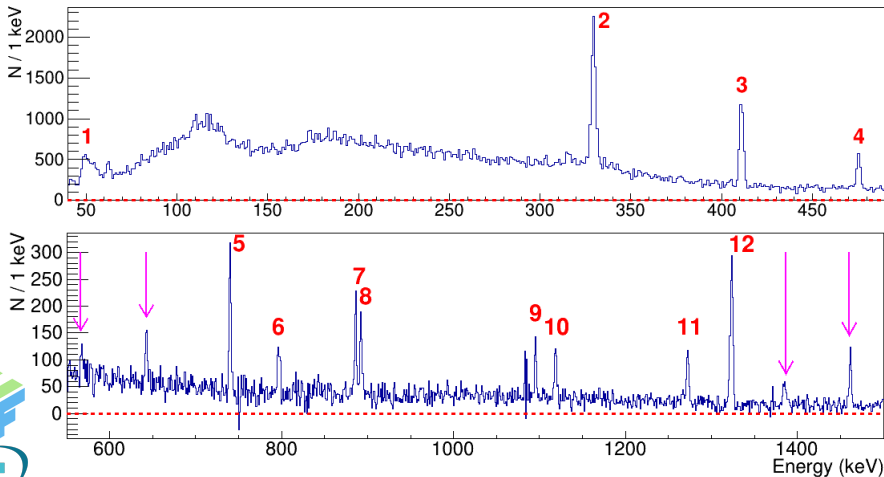


C. Dossat, et al., *Nuclear Physics A* **792**, 18-86 (2007).  
J. Giovinazzo, et al., *Eur. Phys. J. A* **10**, 73-84 (2001).

$\beta$ -delayed proton energy spectra

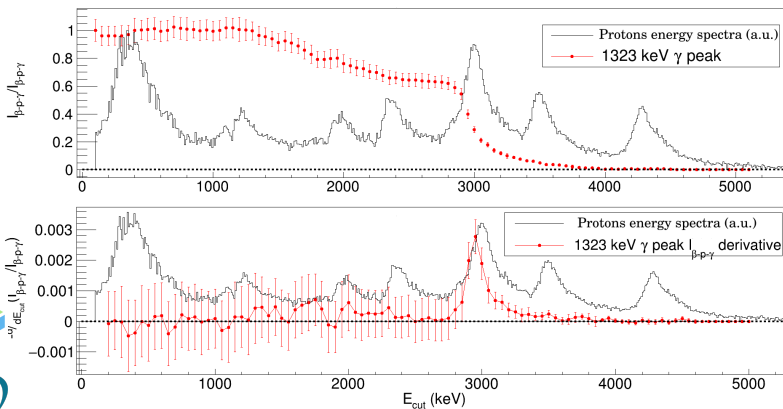
C. Dossat, et al., *Nuclear Physics A* **792**, 18-86 (2007).

A. Ortega, PHD dissertation, Université de Bordeaux (2023).

$\beta$ -delayed  $\gamma$  energy spectra

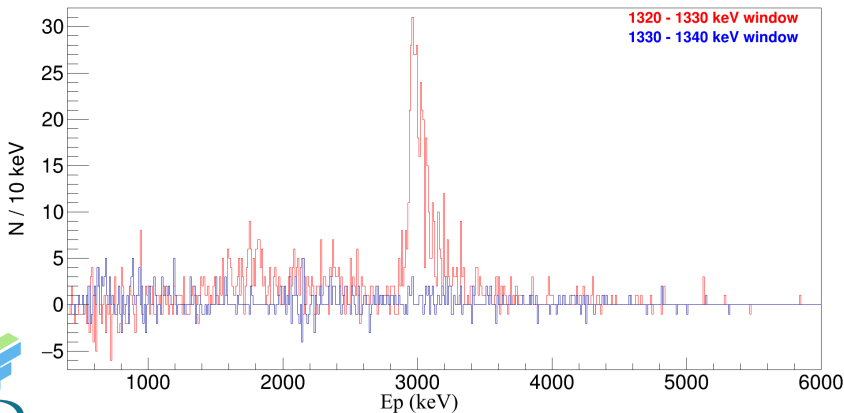
## Study of $p$ - $\gamma$ coincidences for the $\gamma$ 1323 keV with a novel data analysis methodology

We also studied the variation of the 1323 keV  $\gamma$ -peak intensity by applying energy thresholds ( $E_{\text{cut}}$ ) to the charged particle energy spectra (top panel), and then calculating its numerical derivative (bottom panel):



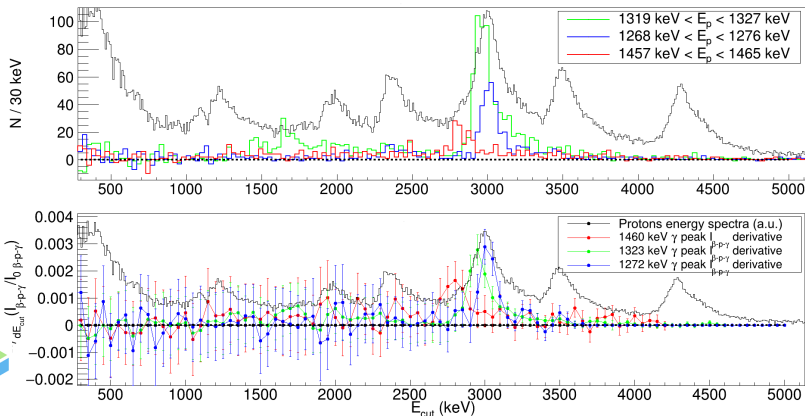
# Study of $p$ - $\gamma$ coincidences using a traditional data analysis, gating in the 1323 keV $\gamma$

Charged particle spectra gating in the 1323 keV gamma.

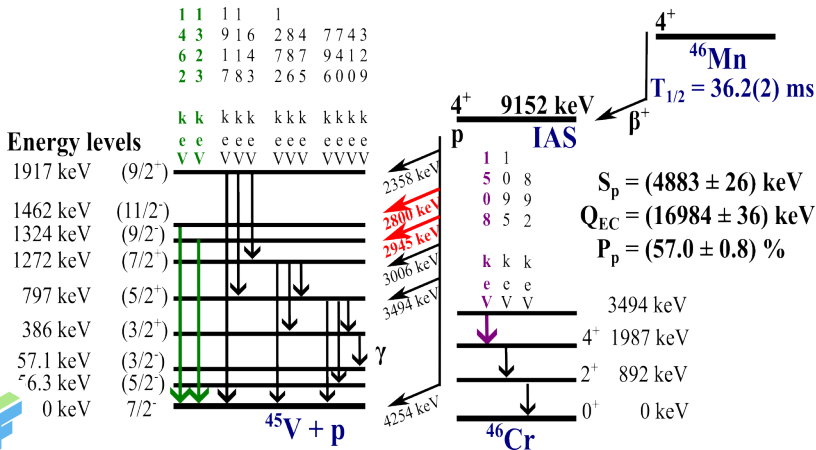


# Study of $p$ - $\gamma$ coincidences for the 1323, 1272, and 1462 keV $\gamma$ s

Charged particle spectra gating in the 1323, 1272, and 1462 keV  $\gamma$ s:



## $^{46}\text{Mn}$ decay with new insights



## Conclusions and future work

- Energy spectra for charged particles (protons and betas) (200-5600 keV) and photons (40-500 keV and 550-1500 keV) related to the  $^{46}\text{Mn}$   $\beta$ -decay were obtained. Those spectra are compatible with J. Giovinazzo, et al. and Dossat, et al. results, **with greater statistics than previous experiments.**
- A novel experimental data analysis is presented, whose results are corroborated by a different method. Results allow us to identify 2 new proton emissions in the  $^{46}\text{Mn}$   $\beta$ -decay scheme.
- Next steps of the analysis:
  1. To identify relevant contributions, if any, to the  $^{45}\text{V}(p,\gamma)^{46}\text{Cr}$  reaction rate due to narrow isolated resonances.
  2. To apply Shell Model, also looking into the mirror nuclei  $^{46}\text{Ti}$ , to access to presently unknown excited states in  $^{46}\text{Cr}$ .



## Thanks for your attention!

- This work is partially supported by DGAPA-UNAM IG101423, CONACyT 314857, MICIU PID2023-147569NB-C21, and MICIU PID2023-147569NB-C22 projects.
- This work was supported by the European Union's Horizon 2020 Framework research and innovation programme 654002 (ENSAR2) and by the Conseil Régional d'Aquitaine, France.
- We thank the support from ASTRA-NUCAP, and the Centro de Estudios Avanzados en Física, Matemáticas y Computación of the University of Huelva, CEAFCM-UHU.



Special thanks to **EuNPC 2025** organizers for making this talk possible.



Universidad  
de Huelva



## Efficiency evaluation for $\beta$ and $\gamma$ detection

### $\gamma$ detection efficiency of HPGe clovers

- The peaks of the  $\gamma$ -calibration sources were used:  $^{56+60}\text{Co}$ ,  $^{207}\text{Bi}$ , and  $^{133}\text{Ba} + ^{137}\text{Cs}$ .
- The efficiency in each peak was found using the equation:

$$\varepsilon_{\gamma} = \frac{N_{\gamma} * \text{Div}}{I_{\gamma} AT_{\text{run}}(1 - \tau)}$$

- Then we fit the following function  $f(E) = \exp a + b \ln E$  to get the  $\gamma$  efficiency detection at any energy value.

### $\beta$ detection efficiency of DSSSD strips

- We used the decay curves of the pure  $\beta$  emitters:  $^{46}\text{Cr}$  and  $^{42}\text{Ti}$  (within the cocktail beam).
- While doing the exponential fit, the total number of  $\beta$ s detected by the DSSSD strips  $N_{\beta}$  was counted.
- Then the  $\beta$  detection efficiency was obtained following the equation:

$$\varepsilon_{\beta} = \frac{N_{\beta}}{N_{\text{imp}}(1 - \tau)}$$



## Peak intensities

### Measuring $\beta - \gamma$ intensities

- To measure the  $\beta - \gamma$  intensities of the  $\gamma$  peaks we use the equation:

$$I_{\beta,\gamma} = \frac{N_{\gamma}}{\varepsilon_{\beta} * \varepsilon_{\gamma} * N_{\text{imp}} * (1 - \tau)},$$

- where  $N_{\gamma}$  stands for the number of  $\gamma$ s detected,  $N_{\text{imp}}$  for the number of implantation events,  $\tau$  for the dead time,  $\varepsilon_{\beta}$  for the  $\beta$  detection efficiency, and  $\varepsilon_{\gamma}$  for the  $\gamma$  detection efficiency.

### Measuring proton- $\gamma$ intensities

- In the case of the p- $\gamma$  intensities, we use the equation:

$$I_{p,\gamma} = \frac{N_{\gamma}}{\varepsilon_{\gamma} * N_{\text{imp}} * (1 - \tau)},$$

- where  $\varepsilon_p$ , the proton detection efficiency, can be considered as 1 for protons with  $E_p < 4$  MeV.



E. A. Orrigo, et al., *Physical Review C* **93**, 044336 (2016).

- Table obtained from L.-S. The, et. al., ApJ 504, 500-515 (1998).

TABLE 5  
ORDER OF IMPORTANCE OF  
REACTIONS PRODUCING  
 $^{44}\text{Ti}$  AT  $\eta = 0^a$

Reaction	Slope
$^{44}\text{Ti}(\alpha, p)^{47}\text{V}$ .....	-0.394
$\alpha(2x, \gamma)^{12}\text{C}$ .....	+0.386
$^{45}\text{V}(p, \gamma)^{46}\text{Cr}$ .....	-0.361
$^{40}\text{Ca}(\alpha, \gamma)^{44}\text{Ti}$ .....	+0.137
$^{57}\text{Co}(p, n)^{57}\text{Ni}$ .....	+0.102
$^{36}\text{Ar}(\alpha, p)^{39}\text{K}$ .....	+0.037
$^{44}\text{Ti}(\alpha, \gamma)^{48}\text{Cr}$ .....	-0.024
$^{12}\text{C}(\alpha, \gamma)^{16}\text{O}$ .....	-0.017
$^{57}\text{Ni}(p, \gamma)^{58}\text{Cu}$ .....	+0.013
$^{58}\text{Cu}(p, \gamma)^{59}\text{Zn}$ .....	+0.011
$^{36}\text{Ar}(\alpha, \gamma)^{40}\text{Ca}$ .....	+0.008
$^{44}\text{Ti}(p, \gamma)^{45}\text{V}$ .....	-0.005
$^{57}\text{Co}(p, \gamma)^{58}\text{Ni}$ .....	+0.002
$^{57}\text{Ni}(n, \gamma)^{58}\text{Cu}$ .....	+0.002
$^{54}\text{Fe}(\alpha, n)^{57}\text{Ni}$ .....	+0.002
$^{40}\text{Ca}(\alpha, p)^{43}\text{Sc}$ .....	-0.002

<sup>a</sup> Order of importance of reactions producing  $^{44}\text{Ti}$  at  $\eta = 0$  according to the slope of  $X(^{44}\text{Ti})$  near the standard reaction rates.



## Sensitivity of $^{44}\text{Ti}$ and $^{56}\text{Ni}$ Production in Core-collapse Supernova Shock-driven Nucleosynthesis to Nuclear Reaction Rate Variations

Shiv K. Subedi<sup>1</sup>, Zach Meisel<sup>1</sup>, and Grant Mezz<sup>1</sup>

Institute of Nuclear & Particle Physics, Department of Physics & Astronomy, Ohio University, Athens, OH 45701, USA; [ss383615@ohio.edu](mailto:ss383615@ohio.edu), [meisel@ohio.edu](mailto:meisel@ohio.edu)  
Received 2020 February 25; revised 2020 May 16; accepted 2020 May 26; published 2020 July 16

### Abstract

Recent observational advances have enabled high resolution mapping of  $^{44}\text{Ti}$  in core-collapse supernova (CCSN) remnants. Comparisons between observations and models provide stringent constraints on the CCSN mechanism. However, past work has identified several uncertain nuclear reaction rates that influence  $^{44}\text{Ti}$  and  $^{56}\text{Ni}$  production in postprocessing model calculations. We evolved one-dimensional models of  $15 M_{\odot}$ ,  $18 M_{\odot}$ ,  $22 M_{\odot}$ , and  $25 M_{\odot}$  stars from zero age main sequence through CCSN using Modules for Experiments in Stellar Astrophysics and investigated the previously identified reaction rate sensitivities of  $^{44}\text{Ti}$  and  $^{56}\text{Ni}$  production. We tested the robustness of our results by making various assumptions about the CCSN explosion energy and mass cut. We found a number of reactions that have a significant impact on the nucleosynthesis of  $^{44}\text{Ti}$  and  $^{56}\text{Ni}$ , particularly for lower progenitor masses. Notably, the reaction rates  $^{13}\text{N}(\alpha, n)^{16}\text{O}$ ,  $^{17}\text{Fe}(\alpha, n)^{20}\text{Ne}$ ,  $^{52}\text{Fe}(\alpha, n)^{55}\text{Co}$ ,  $^{58}\text{Ni}(\alpha, n)^{61}\text{Cu}$ ,  $^{57}\text{Ni}(\alpha, n)^{57}\text{Co}$ ,  $^{56}\text{Cr}(\alpha, n)^{59}\text{Ni}$ .

- Not  $^{45}\text{V}(p, \gamma)^{46}\text{Cr}$ , but  $^{47}\text{V}(p, \gamma)^{48}\text{Cr}$ !
- $^{39}\text{K}(p, \gamma)^{40}\text{Ca}$  and  $^{39}\text{V}(p, \alpha)^{36}\text{Ar}$  also affect  $^{44}\text{Ti}$  abundancy.

- $^{44}\text{Ti}$  is produced when a shock-wave after the core-collapse reaches the  $\alpha$ -rich region in the cooling phase ( $1 < T_9 < 5$ ).

- As  $\vec{J} = \vec{\ell} + \vec{j}_1 + \vec{j}_2$  and  $\Pi = \pi_1 \pi_2 (1)^{-\ell}$ , for  $^{45}\text{V} + p \rightarrow ^{46}\text{Cr}^*$  and only considering  $\ell = 0, 1$  resonant capture then the candidates for resonances are:

$$J^\pi(^{45}\text{V}_{\text{gs}}) = 7/2^-; \quad J^\pi(p) = 1/2^+ \Rightarrow J^\pi(^{45}\text{V}_{\text{gs}}) = 2^+, 3^+, 4^+, 5^+, 3^-, 4^-$$

- On the other hand, allowed  $\beta$ -decay transitions follows:

$$\Delta J = 0; \quad \pi_i = \pi_f \quad \text{for Fermi}$$

$$\Delta J = 0, 1; \quad \pi_i = \pi_f \quad \text{for Gamow-Teller}$$

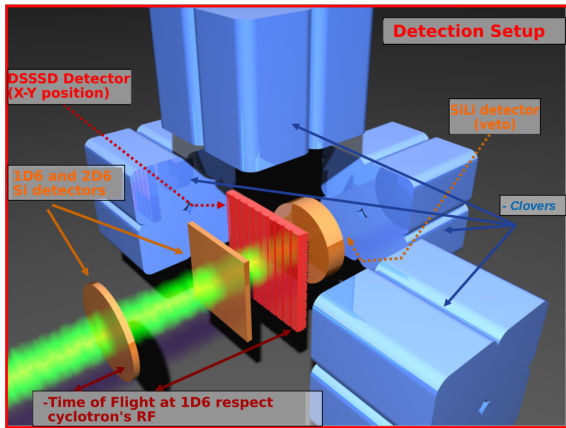
As  $J^\pi(^{46}\text{Mn}_{\text{gs}}) = 4^+$  and considering only allowed transitions:

$J^\pi(^{46}\text{Cr}^*) = 3^+, 4^+, 5^+$  ( $2^+, 3^-$  and  $4^-$  could be sufficiently populated but they are strongly inhibited).



## Detection setup

- The primary beam was a  $^{58}\text{Ni}^{26+}$  at 74.5 MeV/u, which collided with a 230.6 mg/cm<sup>2</sup> thick  $^{\text{nat}}\text{Ni}$  target.
- With the LISE separator elements, the isotopes to be implanted in the detectors array were selected.
- The detectors array used during the experiment is shown:

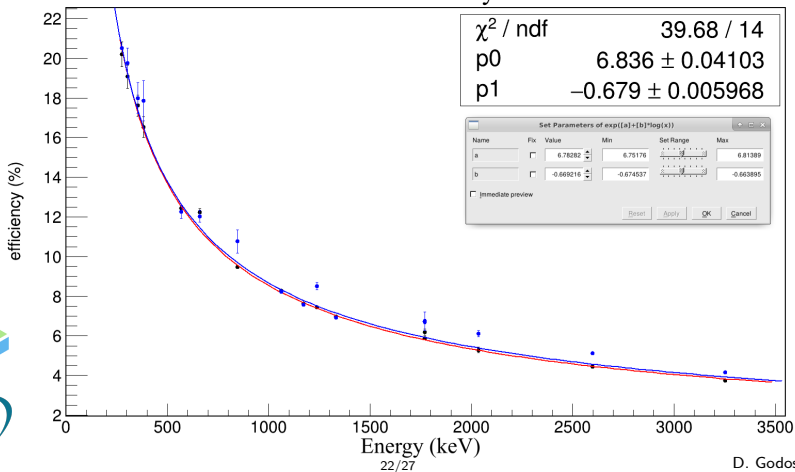


## Gamma efficiency curve

The gamma efficiency curve obtained for the analysis is shown in the next figure:

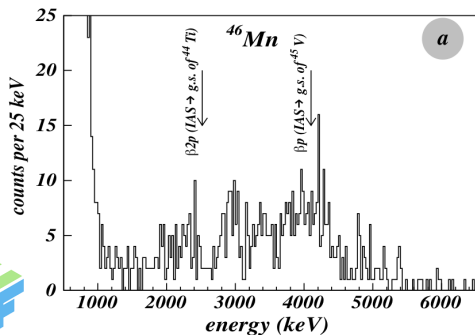
:

### Gamma efficiency curve

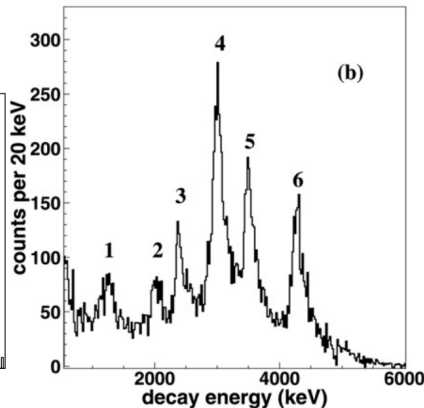


## Charged particle spectra

The charged particle spectra obtained by Dossat and Giovinazzo are presented:



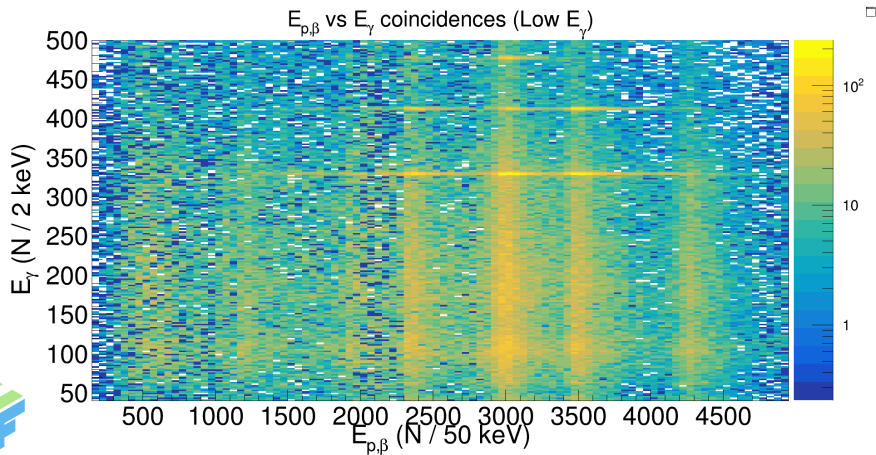
(c)



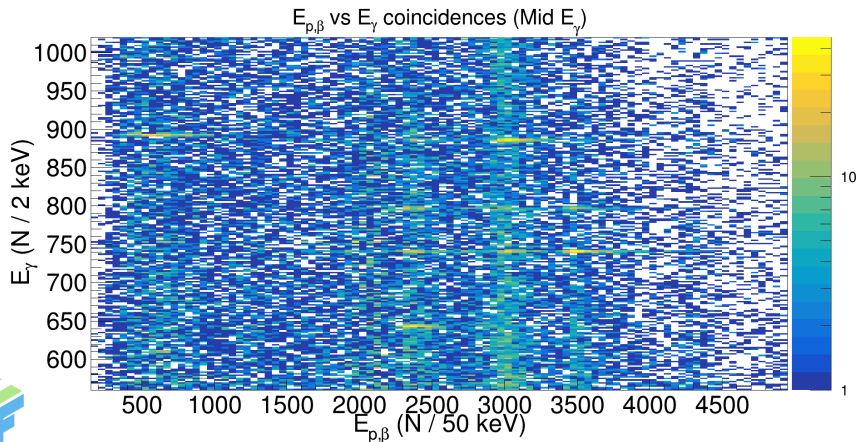
(d)



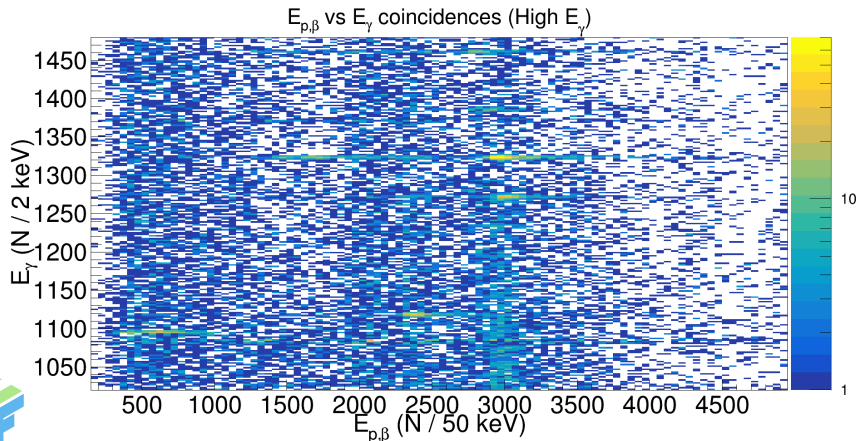
## $p$ - $\gamma$ coincidences for 40-500 keV $\gamma$ 's



## $p$ - $\gamma$ coincidences for 550-1020 keV $\gamma$ 's



## $p\text{-}\gamma$ coincidences for 1020-1480 keV $\gamma$ 's



## $p$ - $\gamma$ coincidences for 1480-1940 keV $\gamma$ 's

